10.2478/msr-2013-0033

MEASUREMENT SCIENCE REVIEW, Volume 13, No. 4, 2013

Numerical Analysis of Influencing Factors and Capability for Thermal Wave NDT in Liquid Propellant Tank Corrosion Damage Detection

Jin Guofeng, Zhang Wei, Shi Jun, Yang Zhengwei, Hu Yu, Huang Zhiyong, Tian Gan

602 office, Xi'an Research Institute of High Technology, Hongqing Town, Xi'an 710025, China, douhao616@126.com

Due to the disadvantages of traditional NDT methods for liquid propellant tank corrosion detection, Thermal Wave Nondestructive Testing (ITWNDT) technology was applied. The heat exchange process of thermal wave in corrosion tank was simulated by the numerical method. Parameters of TWNDT as the best detection time (t_{best}), the maximum surface temperature difference (ΔT_{max}), and the temperature difference holding time ($\tau_{\Delta T>0.1}$) were discussed as the targets. Based on these parameters, factors influencing the detection results of tank materials, dressed liquid (also considered as the corrosion product), pit characters (depth and size), heat flux and thermal excitation time length (pulsed width), environmental conditions and other factors were analyzed. Simulation results show that ITWNDT can identify the defect depth, size and position rapidly and effectively. Material properties of the tank were influencing the t_{best}, ΔT_{max} and $\tau_{\Delta T>0.1}$, while the dressed liquid, thermal excitation parameters and the conditions of environment do not influence the t_{best}. Pit characters of the depth and size have close relationship with t_{best} and ΔT_{max}, therefore, for a tank with certain material and certain liquid dressed in, the pit corrosion damage can be accurately evaluated.

Keywords: Liquid propellant tank, corrosion, infrared thermal wave detecting, influencing factors, numerical simulation.

1. INTRODUCTION

CORROSION is a common injury for varieties of large-scale liquid and gas tanks, especially in petroleum chemical engineering and aerospace areas. Corrosion decreases wall thickness and strength, and serious corrosion will lead to leakage, which is dangerous for not only bringing economic loss, but also environmental pollution and personnel incidents. Measurements are necessary to grasp the performance of the tank, in which the corrosion damage detection is an important factor. Methods commonly used in corrosion detection are ultrasonic, eddy current, magnetic flux leakage, etc. In recent years, the development of new technologies, such as acoustic emission and ultrasonic C-scan, has improved the level of corrosion detection [1]-[4]. However, as commonly recognized, some limitations of these technologies make the detection results unsatisfactory for the demand for high efficiency, non-destructive, non-contact, on-line and accurate detection. Therefore, fast and efficient corrosion detection method becomes an urgent need to meet the problem.

Infrared thermal wave non-destructive technology (ITWNDT) has been developed in recent years as a fast, accurate, non-destructive testing technology. Some advantages of ITWNDT as intuitive test results, single-sided testing, non-contact, large area detection and quantitative detection were successfully applied in the aerospace, power generation, automotive, construction and other fields [5]-[10]. S. Marinetti [11]-[12], E. Grizato [13]-[14], D. Ambrosini [15], M. Jonsson [16] and Yang Jing [17] studied the application of ITWNDT in corrosion detection, and achieved relatively good results. Notwithstanding this, the influence factors in the thermal Wave NDT are still not completely exploited. Therefore, a numerical simulation method is used in this paper for calculating the heat transfer process in thermal wave detection. With the simulation results, factors that influence the detection of propellant tank corrosion are analyzed, and the quantitative relationship between defect detection parameters is established, which are the foundation for the detection of propellant tank corrosion damage.

2. INFRARED THERMAL WAVE NONDESTRUCTIVE TESTING TECHNOLOGY

2.1. Basic principle of ITWNDT

The basic principle of ITWNDT is the law of thermal conduction and radiation [18]. The principle map is shown in Fig.1. Imposed by the thermal excitation, the heat flux is produced and conducted to the tank wall. When the thermal wave is transmitted to the corrosion surface, part of the thermal wave is reflected back and transmitted in the opposite direction until the surface of the tank, where the thermal wave reflects again. And then, following the same patterns of cycle of transition and reflection, the heat flux will decay completely. The surface temperature field distribution at the corrosion area is formed by the attenuation of surface temperature and the accumulation of the constant reflection from the corrosion surface. Therefore, by controlling the thermal excitation and applying an infrared camera to monitor the surface temperature fields, information of the corrosion inside the structure can be obtained.

2.2. Parameters of the detection capability

Usually, the detection capability of ITWNDT is characterized by three parameters as [16], [19]: the surface temperature difference $\Delta T(t)= T_d(t)-T_s(t)$, here t is the time, T_d and T_s are the surface temperatures over corrosion damage and sound area, respectively; the best detection time t_{best}, which is the time when the surface temperature difference is up to the maximum; and the best detection sensitivity A is the ratio between the maximum $\Delta T(t)$ and the

average surface temperature. Here, the surface temperature difference captured by the infrared camera is the most important one, because the minimum surface temperature difference that can be captured depends on the sensitivity of the camera, and the other two parameters can be obtained from the surface thermal image sequences. The defects can be effectively evaluated by analyzing relationships of the three parameters with the detection results.

In addition, because of the limitation of the thermal image acquisition frequency (currently, the acquisition frequency is a few Hz to tens of Hz), the time length of surface temperature difference should be longer than the time of the camera sensitivity to ensure that the camera has recorded the temperature difference information. This time length is called temperature difference holding time and is expressed as $\tau_{\Delta T>0.1}$ in this paper. The bigger the $\tau_{\Delta T>0.1}$ is, the more favorable is the camera capturing the damage information. According to the current performance of infrared detection equipment, the thermal sensitivity of the camera is set to 0.1 ℃ and the image acquisition frequency is set to 50 Hz in this paper, which means that the detection capability and the detection effectiveness are discussed by ΔT>0.1 ℃ and $\tau_{\Delta T>0.1} \geqslant 0.02$ s.

3. Modeling and Computation

3.1. Morphology assumption for tank corrosion damage

Different corrosion pit morphology is generated in different tank materials in different corrosive environmental conditions. Thus, the scholars have different opinions of the shape of the pits, and the pits are equivalent for a variety of shapes, such as pinhole-shaped, conical, cylindrical, spherical cap-shaped and ellipsoidal. Commonly, considering the complex modeling of conical, spherical cap-shaped ellipsoidal pits in the finite element model, pits are often equivalent to the cylindrical shape with the same pit volumes in the finite element simulation calculation [20]. Following this way, the corrosion hole in the cross section is assumed in this paper as shown in Fig.1., where h is the tank wall thickness, D is the corrosion hole diameter, Δh is pit depth, d is the remaining wall thickness.

When applying the ITWNDT to detect the corrosion, researchers often do not consider the corrosion products or dressed liquid in the tank [12], [17]. In order to accurately obtain the corrosion detection results, in particular to study the detection of in-service tank, material properties of corrosion products were set in the paper's calculation.

3.2. Models of calculation

Generally, the differential equations of heat conduction inside the material are complexly expressed, with the complex initial and boundary conditions, it is difficult to solve such a problem of taking into account the presence of corrosion product or dressed liquid, while an analysis based on the finite element method is an effective way to solve this problem. And yet, specimens of tank with the dimensions of 0.25 × 0.15 × 0.005 m are established in ABAQUS. All the specimens have different corrosion of various pit depth, diameter or corrosion products at the inside tank wall surface. Parameters of the calculation models are shown in Table 1. In the following analysis, all simulations are calculated on the model 1, except the simulation for the pit depth calculation which is done on the model 2, and the data are all extracted from the outside surface center over the 20 mm pitting damage.

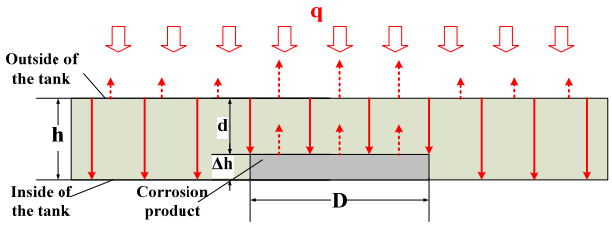

Fig.1. Basic principle of ITWNDT for corrosion detection.

Table 1. Model parameters.

Parameter	Model 1					Model 2				
D (mm)	2	5	10	20	30	20	20	20	20	20
Δh (mm)	2	2	2	2	2	0.5	1	1.5	2	2.5
h (mm)	5	5	5	5	5	5	5	5	5	5

In the simulation, assume the ambient temperature T_e remains unchanged, there is no internal heat source, and ignore the convection and radiation at the side. Because thermal excitation time and detection time are short enough, it can be assumed they have no phase and thermophysical properties (including specific heat, density, thermal conductivity, etc.) change of the liquid. Selected grid cell is DC3D8 eight-node linear heat transfer hexahedral element, so that the calculation model of the node is less than tetrahedral element, and can get high calculation accuracy [21]. The sweep meshing method is used to ensure that the division of the grid is uniform in the thickness direction, and to reduce the grid non-uniformity caused by calculation errors.

Commonly used stainless steel and high strength aluminum alloy material in liquid propellant tank are studied in the simulation, the material parameters are shown in Table 2. [22]. Where ρ is the density (Kg/m^3); λ is the heat transfer coefficient, W/m·℃; C is specific heat, J/Kg·℃.

Testing conditions set in the models are shown in Table 3. According to the factor analyzed in each simulation, its value is only changed in the calculation, with other conditions set as Table 3. shows. Where h_c is the convective heat transfer coefficient of environment, W/m^2·℃; T_e is the environment temperature, ℃; q is the heat flux, J/m^2; τ_b is the time length of pulse thermal stimulation (referred to as pulse width), s.

Table 2. Physical parameters of materials in calculation models.

Conditions		ρ	C	λ
Material of tank	Stainless steel	7801	473	43
	Aluminum alloy	2610	904	107
Liquid in the tank (or corrosion product)	Propellant	1446	1472.8	0.1492
	Air	1.0	1005	0.0251
	Water	1000	4200	0.58
	Oil	888	1880	0.145
	Liquid NH_3	610.4	4758	0.4792

Table 3. Testing conditions.

Tank material	As the product	Environment	Testing
Stainless steel	Air	h_c=10 T_e=20	q=5×10^7 τ_b=0.002

3.3. Calculation for the model

The calculation process of pulse thermal wave detection can be divided into two steps:

The first step (the transient heating process): t=0 s~0.002 s

Initial condition: $T\big|_{t=0}=T_e$ (1)

Boundary conditions:

$$\begin{cases} q=-\lambda\dfrac{\partial T}{\partial z}\Big|_{z=0.005}=q_0 \\ k\dfrac{\partial T}{\partial z}\Big|_{z=0}=-h_c\left(T-T_e\right) \end{cases} \quad (2)$$

Assumed side of the structure is adiabatic.

The second step (the cooling process): t=0.002 s~20 s

Initial condition: Taking the calculation results of the first step

Time step: 0.1 s

Boundary conditions: $k\dfrac{\partial T}{\partial z}\Big|_{z=0}=h_c\left(T-T_e\right)$ (3)

The other conditions are set the same with the first step.

According to the initial and boundary conditions, with the different loading demand, the model is calculated.

3.4. Surface temperature field distribution

Simulation results of surface temperature field distribution for stainless steel tank are shown in Fig.2. It can be seen that 0.1 s after pulse heated, the heat has not spread to the corroded areas, and the surface temperature distribution is uniform. At 0.3 s, four damage pits with larger diameter have been observed through hot spots on the surface. Over the time, the temperature difference between the corroded areas and normal areas is increasing with the hot spot contrast enhancement. So at 0.8 s, all 5 damage pits were observed from the hot spots and at 1.0 s, the contrast of 5 hot spots up to peak value was observed. Due to thermal diffusion, the surface temperature field gradually balancing with the value of ΔT and the contrast of the hot spots gradually reducing, the hot spot of the smallest diameter damage disappeared first. At 11.2 s, the surface temperature distribution becomes balanced and no damage information can be seen from the image. It can thus be said that the thermal wave detection is very fast, only tens of seconds to accurate position of the pits through the hot spots on the surface, while the sizes of the thermal spots can reflect the sizes of the pits, and the test results are relatively straightforward.

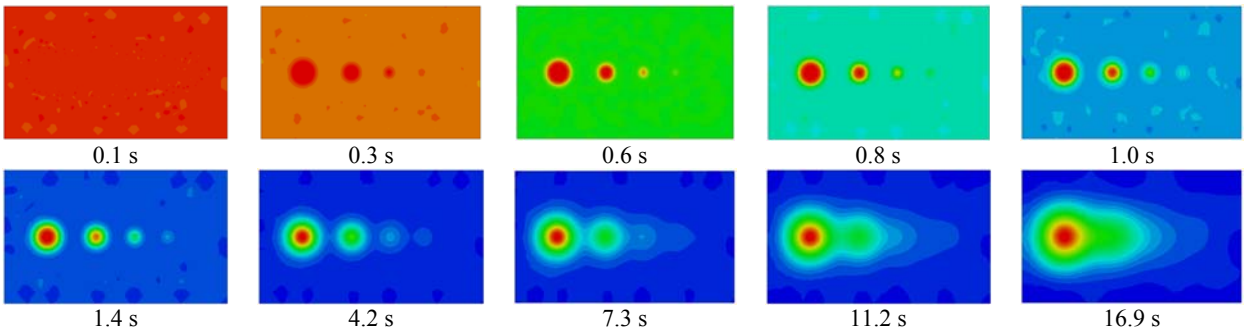

Fig.2 Thermal image sequences of temperature distribution on the surface

4. Analysis of Influencing Factors in Detection

Heat conduction in the tank wall is a complex process, in which there are different heat conduction characteristics caused by different corrosion. Therefore, it is necessary to study the effect of different corrosion damage for detection results to improve the detection capability by ITWNDT. Corrosion morphologies considered here are the wall material, the product (as well as the dressed liquid in the tank), the pit depth, and the pit size. Many factors affect the heat transmission and the surface temperature difference, in addition to damage to its own parameters, the thermal excitation source parameters (about heating method, heat flux and thermal excitation time, etc.), environmental factors (about convective heat transfer, thermal radiation, etc.) also play important influence roles in detecting. Small changes in these factors may lead to the damage information submerged. Therefore, all factors above are studied as numerical simulation in the following part.

4.1. Test results of different wall materials

Surface temperature curves and temperature difference curves of stainless steel tank and aluminum tank are shown in Fig.3., the data are captured from the surface center over the 20 mm pit of model 1 with the same detection parameters. It can be seen that in the same testing conditions, for stainless steel tank, the ΔT_{max} is 3.0519 □, and t_{best} is 1.0 s, $\tau_{\Delta T>0.1}$ is over 20 s; while for aluminum tank, ΔT_{max} is 4.2391 □, t_{best} is 0.3 s, and the $\tau_{\Delta T>0.1}$ is only 16.1 s. But the surface temperatures of the two materials are dropping fast, which makes a short time length of the

temperature difference greater than the thermal imaging instrument sensitivity, and a very short retention time of the maximum temperature difference, which means that the best detection time soon disappears, and therefore higher acquisition frequency of thermal camera is required.

In the same testing conditions, assume the wall materials are copper alloy (ρ = 8922, λ = 22.7, C = 410), nickel-based corrosion resistant alloy (ρ = 8073, λ= 460, C = 12) and magnesium alloy (ρ = 1810, λ = 66, C = 1000) [22] to analyze the influence of wall material on the detection results. The best detection times calculated are 1.9 s, 6.3 s and 5.7 s, respectively. The surface temperature difference history curves of the 5 materials a re shown in Fig.4. The greater the thermal conductivity of the material is, the smaller the results of t_{best} and $\tau_{\Delta T>0.1}$. This is bad for damage detection and recognition. Fitting the thermal diffusivity of the 5 materials with their t_{best} values, we can get such a figure as shown in Fig.5., and they meet the exponential decay relationship expressed as:

$$t_{best} = 0.9\times10^{-4} e^{\frac{-\alpha}{0.38081}} + 4.4517\times10^{-6} \tag{4}$$

Here, α is the thermal diffusivity, $\alpha=\lambda/\rho c$. Seen from (4), the larger thermal diffusivity of the material, the bigger ΔT, but the smaller corresponding t_{best}, which makes the smaller $\tau_{\Delta T>0.1}$, this phenomenon is bad for the detection.

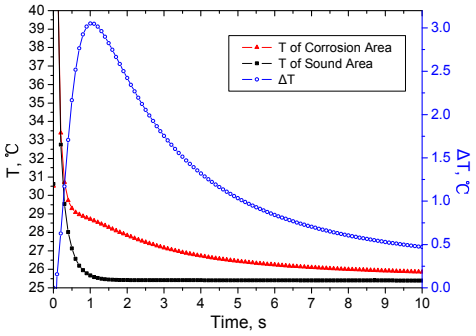

(a) Stainless steel

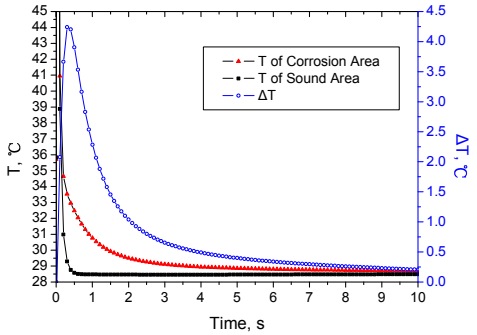

(b) Aluminum alloy

Fig.3. T and ΔT curve of the same corrosion for stainless steel and aluminum alloy tank.

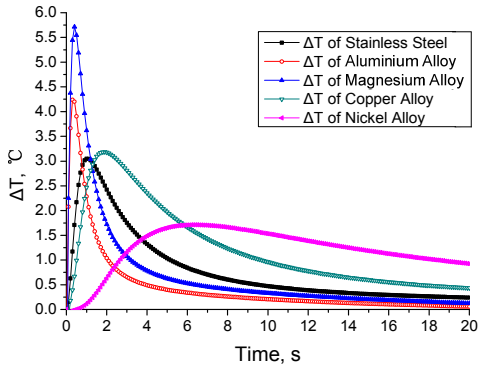

Fig.4. ΔT-t curves of different wall materials.

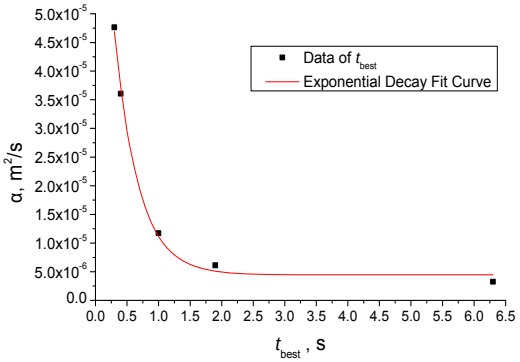

Fig.5. Fitting curve of α against t_{best}.

Testing results of the tank dressed in different liquids are shown in Fig.6., different temperature dropping processes of the liquids appear in Fig.6.(a), the slowest one is air as the product, followed by oil and propellant, the water is the fastest. But we also can see from Fig.6.(b) that liquid has different influence on the testing results with the wall materials, it only influences the value of $T(t)$, but cannot change the value of t_{best}, which means whatever the liquid dressed in, it has the same best detection time. Similarly for ΔT, the largest difference belongs to air, the smallest is water. Because the biggest special heat is water in the 5 materials, more heat is absorbed by water in heat balancing than by other liquids, which makes the thermal wave less reflective at the interface and leads to a smaller temperature difference on the surface, even in later cooling time, negative temperature difference appears. Fitting the ΔT_{max} data with the physical parameters of the products (or dressed liquid), we get expressions (5) and (6), the curves are shown in Fig.6.(c) and Fig.6.(d).

$$\Delta T_{max} = -14.25033\lambda^3 + 14.44036\lambda^2 - 5.6077\lambda + 3.18294 \tag{5}$$

$$\Delta T_{max} = -2.57082\times10^{-7}\rho C + 3.07125 \tag{6}$$

It can be seen that ΔT_{max} and liquid thermal conductivity are in a cubic polynomial relationship, the greater the thermal conductivity of the liquid, the smaller ΔT_{max}. While ΔT_{max} and the density multiply specific heat of a linear relationship, and the bigger density multiply specific heat, the greater the ability of liquid to absorb heat, thereby ΔT is decreased by the reduction of the thermal wave reflection at the interface.

The ΔT_{max} of stainless steel tank dressed in propellant is 2.5763 ℃, and t_{best} is 1.0 s, $\tau_{\Delta T>0.1}$ is 13.7 s, so we can use the infrared thermal wave method to detect the inside corrosion of in-severe liquid propellant tank.

4.2. Influences of the corrosion pit characteristics

The depth and size of the pits are important parameters for evaluating the corrosion degree [2], [20], which is the basis of the assessment of the structure life and safety. Fig.7. shows the calculation results of corrosion damage with the same diameter and different depths. Fig.8. shows the calculation results of corrosion damage with the same depth and different diameters.

Basically, the same surface temperature trend for testing different depth pits is seen in Fig.7. By the interaction of the thermal wave reflection in the horizontal and the thermal diffusion, small protrusions appeared in the cooling process of deep pits, as seen in Fig.7.(a), while the surface temperature of the shallow pit area is close to the surface temperature of the normal region, the result reflects the complexity of the heat transfer. ΔT_{max} is proportional to the pit depth as shown in Fig.7.(b), the deeper are the pits, the greater is the surface temperature difference, and the easier for damage to be detected. The ΔT_{max} and pit depth meet the exponential growth curve fitting relation expressed as:

$$\Delta T_{max} = 1.12067 e^{\frac{a}{1.5343}} - 1.00549 \tag{7}$$

The exponential decay curve fitting relation of t_{best} and the pit depth is expressed as:

$$t_{best} = 0.93194 e^{-\frac{a}{3.3496}+0.50111} \tag{8}$$

For the corrosion pit of 0.5 mm depth, ΔT_{max}=0.4830 ℃, t_{best} =1.3 s, $\tau_{\Delta T>0.1}$=11.5 s, and yet, at the thermal camera sensitivity of 0.1 ℃, it is well detected by ITWNDT. Accordingly, under the condition that the diameter of corrosion is 20 mm, the wall thickness is 5 mm, pit depth of 0.3287 mm can be detected by ITWNDT, and the best detection time is 1.3944 s, which are calculated by (7) and (8), respectively. Therefore, infrared thermal wave technology can detect small corrosion damage.

It can be seen from Fig.8. that the bigger is the pit size, the greater is the maximum surface temperature difference, the longer is the best detection time, and the longer is the temperature difference holding time, the more likely is the damage to be detected. There are small protrusions on the larger diameter pit cooling curve and the cooling is relatively flat, as is shown in Fig.8.(a). It is mainly due to the heat conduction along the thickness direction [19]. For big size pits, there is less heat lost by the thermal diffusion in the reflect heat dissipation, the surface temperature of the pit center has a short keeping time, which is shown in the *T-t* curve as a small protrusion, thereafter, the temperature decreases smoothly.

The fitting of t_{best} against ΔT_{max} about the diameter of the pits meet the exponential growth and the Boltzmann relationship, respectively, as expressed in (9) and (10), and shown in Fig.8.(c) and Fig.8.(d).

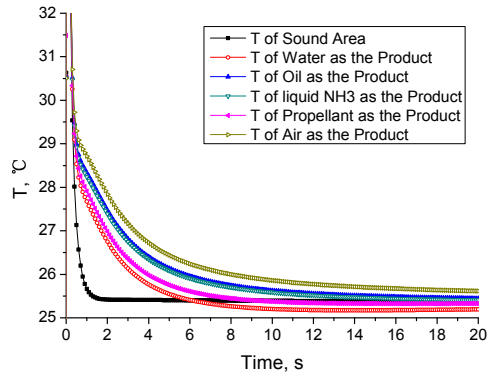

(a) *T* - *t* curves of different corrosion products (liquid)

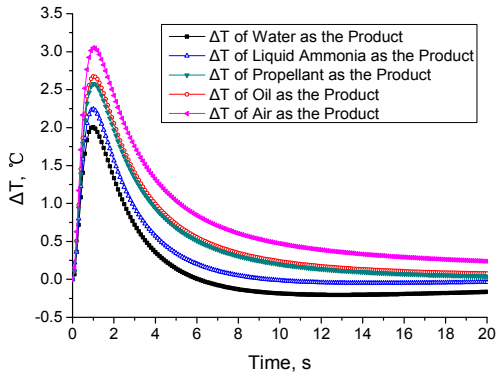

(b) Δ*T* - *t* curves of different corrosion products (liquid)

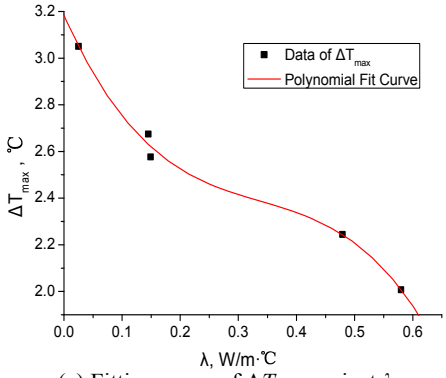

(c) Fitting curve of ΔT_{max} against λ

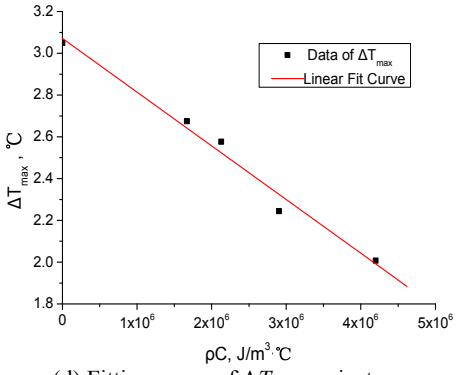

(d) Fitting curve of ΔT_{max} against ρc

Fig.6. *T* and Δ*T* curve of different products at same corrosion.

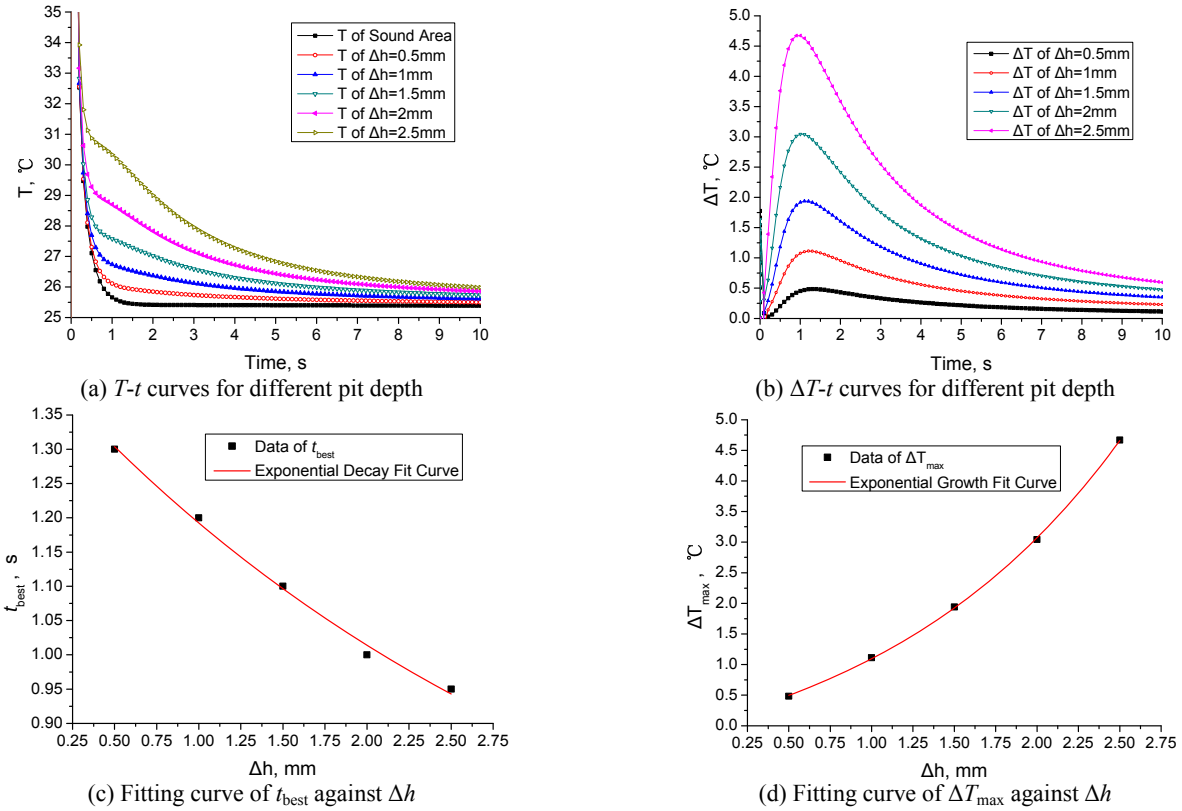

(a) *T-t* curves for different pit depth

(b) Δ*T-t* curves for different pit depth

(c) Fitting curve of t_{best} against Δ*h*

(d) Fitting curve of ΔT_{max} against Δ*h*

Fig.7. Detection results of different corrosion pit depth.

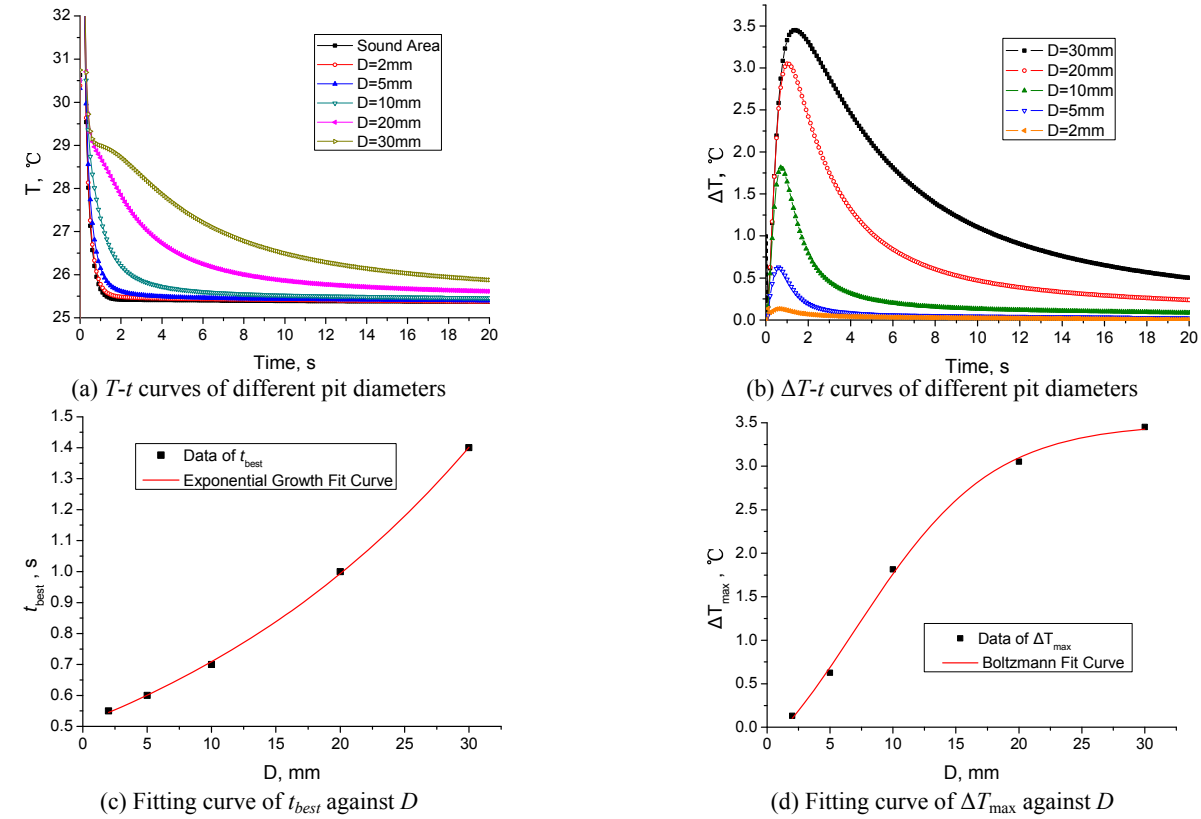

(a) *T-t* curves of different pit diameters

(b) Δ*T-t* curves of different pit diameters

(c) Fitting curve of t_{best} against *D*

(d) Fitting curve of ΔT_{max} against *D*

Fig.8. Detection results of different corrosion pit sizes.

$$t_{best} = 0.45537 e^{\frac{D}{27.67697}+0.05544} \quad (9)$$

$$\Delta T_{\max} = 3.49168 - \frac{4.73476}{e^{\frac{D-7.01002}{5.51587}}+1} \quad (10)$$

According to the thermal camera sensitivity is 0.1 □ for a tank of wall thickness of 5 mm, when the condition of the pit depth is 2 mm, the minimum diameter of the pits that can be detected by ITWNDT is 1.9003 mm, and the best detection time is 0.5155 s, which are calculated by (10) and (9) indicating that the ITWNDT is capable of detecting small corrosion damage.

4.3. Thermal excitation source parameters on the test results

Described pulsed thermal excitation source performance parameters are the heat flux and thermal excitation time length (pulse width, τ_b). Consequently, varying the heat flux and pulse width for numerical calculation, the results are shown in Fig.9.

It can be seen from Fig.9. that under different heat flux and pulse width, the best detection time is 0.1 s and it has no varying, which means that the thermal excitation parameters take no effect on the best detection time. However, the maximum surface temperature difference is proportional to the heat flux and pulse width, the stronger the heat flux and the longer the pulse width, the greater $\Delta T_{\max}$, and the easier damage detection. Fitting the data of $\Delta T_{\max}$ with q and τ_b respectively, we get:

$$\Delta T_{\max} = 6.15524 \times 10^{-8} q - 0.00802 \quad (11)$$

$$\Delta T_{\max} = 1540.10137 \tau_b - 0.01388 \quad (12)$$

Accordingly, the stronger is the heat flux and the longer the pulse width, the bigger is $\tau_{\Delta T>0.1}$ for damage detection. Therefore, optimization of the thermal excitation source parameters will improve the capability of damage detection.

4.4. The impact of environmental conditions

Setting up a series of heat transfer coefficients to calculate the surface temperature distribution under the different environmental convections, the results are shown in Fig.10. The bigger is h_c, the smaller is $\Delta T_{\max}$, the shorter is the $\tau_{\Delta T>0.1}$, but it has little effect on t_{best}, it is because with the increasing of h_c, the heat exchange to environment is sped up, the temperature distribution in the tank wall is rapidly balanced. With the heat transfer coefficient from 1 W/m^2·℃ to 5 W/m^2·℃, $\Delta T_{\max}$ changes from 3.0772 ℃ to 3.0754 ℃, the reduction is 0.0018 ℃. But when h_c changes from 10 W/m^2·℃ to 100 W/m^2·℃, there will be a reduction of 0.0408 ℃, the reduction is 22.5 times of the previous. Therefore, small variety of convective heat transfer coefficient has little influence on the testing result, when the variety is great, the effect cannot be ignored. Taking into account measures such as using a mask, closing door and windows will be beneficial for detection. The fitting relationship of $\Delta T_{\max}$ against h_c is expressed as:

$$\Delta T_{\max} = 3.07763 - 4.49547 \times 10^{-4} h_c \quad (13)$$

Similar with the influence of environmental convection, environmental radiation will also speed up the thermal balance and reduce the surface temperature difference, which all reduce the detection capabilities. According to the Stefan-Boltzmann law and the one-dimensional theory of surface temperature difference formula, the radiation loss of energy is about 1.5 % of the total pulse energy [19]. Generally, because the time used to capture the damage's information is short, there is little energy loss by the radiation and we can ignore it.

Considering the influence of environment temperature, the detection was simulated under the environment temperature of 20 ℃, 25 ℃ and 30 ℃, the calculation results shown there have no effect on the detection because of the same t_{best} and $\Delta T_{\max}$. But in practice, the environment temperature will bring about different environmental convection and environmental radiation, so the testing equipment should be calibrated to the environment temperature to reduce the impact of environmental factors on the test results.

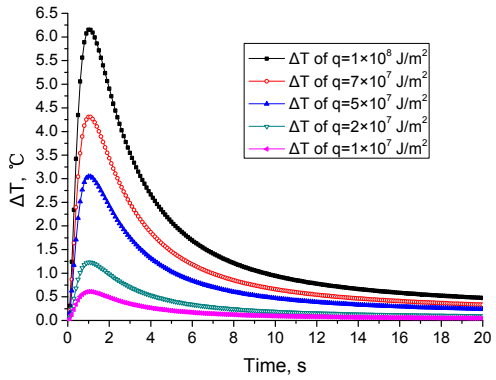

(a) ΔT-t curves of different heat flux

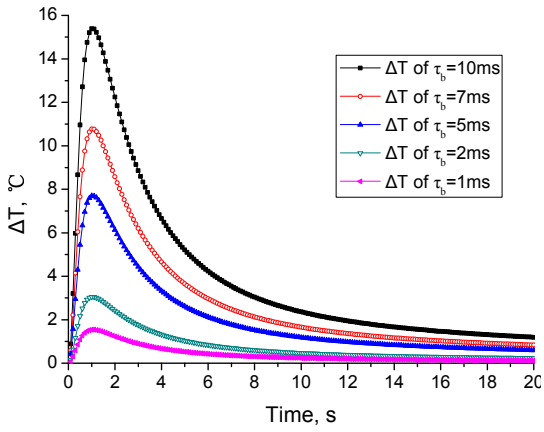

(b) ΔT-t curves of different pulse width

Fig.9. Thermal excitation source parameters on the test results.

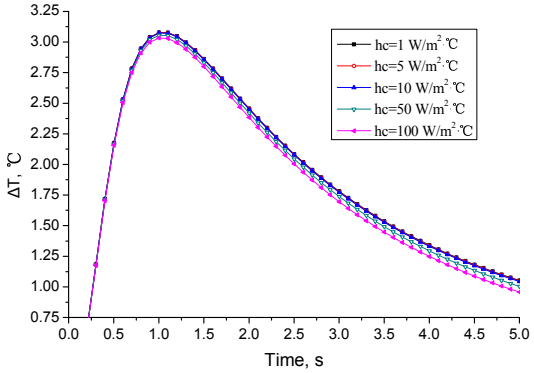

Fig.10. T-t of different convection conditions.

4.5. Discussion

Seen from the simulated detection results above, the ΔT_{max} is generally greater than 0.1 ℃, while the infrared camera temperature resolution is up to 0.01 ℃ now, so the thermal wave technology can fully meet the needs of detection. The analysis of the characterization parameters of ITWNDT from simulation results has shown that:

(1) The best detection time for corrosion damage lies in the material of tank and the characters of corrosion pit, but the corrosion product (dressed in liquid), thermal wave detection parameters and the environment conditions have no influence on t_{bes}. The t_{best} has exponential decay fitting relationship with tank material thermal diffusivity and the corrosion pit depth, and has exponential growth fitting relationship with the pit diameter.

(2) All factors influence ΔT_{max}, while the hot spots on the image are the performance of ΔT, these factors will influence the characteristics of the infrared thermal image and influence the damage identification accuracy. So, the optimization of thermal excitation method, the improvement of environment condition can increase the maximum surface temperature difference for good detection. And there is certain functional relationship between ΔT_{max} and the pit diameter, also the pit depth, by which the corrosion damage can be quantitatively evaluated.

(3) By means of the above analysis, as a parameter of the performance of the relationship of testing equipment's property and the test results, $\tau_{\Delta T>0.1}$ is influenced by several factors. For bigger size and deeper pit, its $\tau_{\Delta T>0.1}$ is longer than the smaller and shallower one, and the corrosion damage can easily be detected. Optimization of the thermal excitation source and improvement of the environment condition can increase the length of $\tau_{\Delta T>0.1}$. Because the data of $\tau_{\Delta T>0.1}$ is captured at the surface center over the corrosion pits, the result can only make clear that the ITWNDT is capable of finding the damage, but the information about the size and depth of the corrosion pit should be acquired by the analysis of t_{best} and ΔT_{max}.

In addition to the above factors, such factors as the resolution and accuracy of the thermal camera, the method of thermal image processing and so on, also influence the corrosion damage detection result. As a result, complex non-linear relationship exists between t_{best} and ΔT_{max} with the above factors, and there is no accurate formula to describe this relationship, it can be described only by effective algorithm to determine the relationship among the parameters. Therefore, this study provides an important reference for getting the quantitative relationship between the various parameters.

5. CONCLUSIONS

Taking into account the various factors influencing the application of infrared thermal wave detection for liquid propellant tank corrosion, by establishing the calculation model of the detection simulation, the following conclusions are obtained:

(1) It is possible to detect the inside corrosion of liquid propellant tank by ITWNDT, and the detection speed is fast, usually only takes a few seconds. With the infrared thermal image sequences as the detection results, the location and size of the corrosion damage can be visually seen.

(2) Parameters such as small thermal diffusivity of the tank material, little thermal conductivity of corrosion product (or dressed liquid), small multiply product of density and specific heat of dressed liquid are good for detection for bigger ΔT_{max} and $\tau_{\Delta T>0.1}$ being captured.

(3) The best detection time and the maximum surface temperature difference have a close relationship with the diameter and depth of the pits. For a certain tank, the characteristics of pits can be accurately evaluated by the acquired t_{best} and ΔT_{max} in the ITWNDT detection. The bigger and deeper pits are more easily to be detected than the smaller and shallower ones.

(4) In permit conditions, increasing the heat flux and pulsed width, and reducing the environment convection and radiation are good for the detection, because the ΔT_{max} and $\tau_{\Delta T>0.1}$ are thus increased. While the environment convection and radiation have little influence on the detection and can be ignored in qualitative analysis, the environment temperature cannot influence the detection result.

ACKNOWLEDGMENTS

We gratefully acknowledge the National Natural Science Foundation of China (No. 51075390, No. 51275518) and Natural Science Basic Research Plan in Shanxi Province of China (No. 2012JQ8018) for support for this project.

REFERENCES

[1] Ni, Y.W., Wang, J.Y., Li, Y. et al. (2009). Corrosion detecting and monitoring technology for metal oil tank. *Oil and Gas Storage & Transportation*, 28 (3), 4-6.

[2] Li, J.Q., Du, C.W. (2007). *Experiment Method and Monitoring Technology for Corrosion*. Beijing: China Petrochemical Press, 240-245.

[3] Wang, W. (2011). Development of corrosion detecting technology for special equipment. *China Special Equipment Safety*, 3, 66.

[4] Ma, J. (2010). Application study of corrosion detection used in the result judgment of salt spray test. *New Technology & New Process*, 8, 98-100.

[5] Maldague, X. (2001). *Theory and Practice of Infrared Technology for Nondestructive testing*. John Wiley & Sons.

[6] Maldague, X. (2002). Introduction to NDT by active infrared thermography. *Materials Evaluation*, 6, 1060-1073.

[7] Wang, X., Jin, W.P., Zhang, C.L. et al. (2004). Infrared thermography NDT methods and development. *Nondestructive Testing*, 26 (10), 497-501.

[8] Sakagami, T., Kubo, S. (2002). Applications of pulse heating thermography and lock-in thermography to quantitative nondestructive evaluations. *Infrared Physics & Technology*, 43, 211-218.

[9] Ibarra-Castanedo, C. (2005). *Quantitative subsurface defect evaluation by pulsed phase thermography: Depth retrieval with the phase*. Ph.D. Thesis, Université Laval, Canada.

[10] Susa, M. (2009). *Numerical modeling of pulse thermography experiments for defect characterisation purposes*. Ph.D. Thesis, Université Laval, Canada.

[11] Marinetti, S., Bison, P.G., Grinzato, E. (2002). 3D heat flux effects in the experimental evaluation of corrosion by IR thermography. In *6th International Conference on Quantitative Infrared Thermography*, 24-27 September 2002. QIRT, 92-98.

[12] Marinetti, S., Vavilov, V. (2010). IR thermographic detection and characterization of hidden corrosion in metals. *Corrosion Science*, 52, 865-872.

[13] Grinzato, E., Vavilov, V. (1998). Corrosion evaluation by thermal image processing and 3D modeling. *Revue Generale Thermique*, 37 (8), 669-679.

[14] Grinzato, E., Vavilov, V., Bison, P.G. et al. (2007). Hidden corrosion detection in thick metallic components by transient IR thermography. *Infrared Physics & Technology*, 49, 234-238.

[15] Ambrosini, D., Paoletti, A., Paoletti, D. et al. (2007). NDT methods in artwork corrosion monitoring. In *O3A: Optics for Arts, Architecture, and Archaeology. Proceedings of SPIE 6618*, 18-21 June 2007. SPIE, 171-179.

[16] Jonsson, M., Rendahl, B., Annergren, I. (2010). The use of infrared thermography in the corrosion science area. *Materials and Corrosion*, 61 (11), 961-965.

[17] Yang, J., Guo, X.W., Dong, S.Q. (2008). Image processing for detection of aluminum alloy with infrared thermographic NDT. *Microcomputer Information*, 24 (1), 55-57, 75.

[18] Yang, Z.W., Zhang, W., Tian, G. et al. (2011). Infrared thermography applied to detect debond defect in shell structure. *Infrared and Laser Engineering*, 40 (2), 186-191.

[19] Yang, Z.W., Zhang, W., Tian, G. et al. (2009). Numerical simulation of influencing factors for thermal wave NDT in composite materials. *Journal of System Simulation*, 21 (13), 3918-3921.

[20] Huang, Y., Zhang, Y., Liu, G. et al. (2010). Ultimate strength assessment of hull structural plate with pitting corrosion damnification under biaxial compression. *Ocean Engineering*, 37, 1503-1512.

[21] Zhan, L. (2007). *Essentials and Examples Explanation of ABAQUS 6.6.* Beijing: China Water Power Press, 117-142.

[22] Dai, G.H. (1999). *Heat Transfer*, 2nd ed. Beijing: Higher Education Press.

Received August 7, 2012.
Accepted July 29, 2013.